System Performances of On-Chip Silicon Microring Delay Line for RZ, CSRZ, RZ-DB and RZ-AMI Signals

Qiang Li, *Student Member, IEEE*, Fangfei Liu, *Student Member, IEEE*, Ziyang Zhang, Min Qiu, *Member, IEEE, Member, OSA*, and Yikai Su, *Senior Member, IEEE, Member, OSA*

***Abstract*—We theoretically study the group-delay characteristics of a silicon microring resonator based on the coupled mode theory, and experimentally demonstrate error-free operations of an on-chip delay line using a silicon-on-insulator (SOI) microring resonator with a 20-μm radius. Four signals of different modulation formats are examined at 5 Gb/s, including return-to-zero (RZ), carrier-suppressed return-to-zero (CSRZ), return-to-zero duobinary (RZ-DB), and return-to-zero alternate-mark-inversion (RZ-AMI). Bit error rate (BER) measurements show that the maximal delay times with error-free operations are 80, 95, 110, and 65 ps, respectively, corresponding to a fractional group delay of $\sim$0.4, $\sim$0.5, $\sim$0.55, and $\sim$0.35. The differences in delay and signal degradations have been investigated based on the signal spectra and pattern dependences. Although the delays are demonstrated in a single ring resonator, the analysis is applicable in slow-light resonance structures such as all-pass filters (APF) and coupled resonator optical waveguides (CROW).**

***Index Terms*—Delay line, microring resonator, modulation format, silicon photonics.**

I. Introduction

ON-CHIP optical delay line has attracted considerable interest due to its potential applications in future optical interconnections and packet-switching systems for data buffering and synchronization [1]–[5]. Coupled resonator structure (CRS)-based delay lines [6], [7] are attracting interests in terms of integration, design flexibility and footprint. Such a structure was implemented in polymer [8], silicon oxynitride (SiON) [9] and silica [10]. However, the relatively small index contrasts in these materials result in comparatively large sizes of the devices. Silicon-on-insulator (SOI) structure has been proved to be an excellent candidate platform for integrated photonics due to its maturity in the electronics industry. The high index contrast of the silicon waveguide allows strong light confinement at the diffraction limit and dramatic scaling of the device size [11]–[15]. The exploitation of resonances based on SOI structure is expected to outperform other slow-light media in terms of miniaturization and on-chip integration. By cascading 56 SOI-based ring resonators in all-pass filter (APF) configuration, a delay exceeding 500 ps with a footprint below 0.09 mm^2 has been demonstrated [16].

On the other side, the past decades have witnessed tremendous improvement in advanced modulation formats for the state-of-the-art communication systems to provide superior performances and meet diverse requirements [17]–[20]. However, there are few publications addressing the delay and signal quality characteristics of diverse modulation formats through slow-light delay lines [21]. To date, system performance of bit error rate (BER) for high-data-rate signals through CRS slow-light delay line was investigated only in the case of non-return-to-zero (NRZ) format [16]. In this paper, we study the system performances of an on-chip delay line based on the silicon micro-ring resonator for different modulation formats, including return-to-zero (RZ), carrier-suppressed return-to-zero (CSRZ), return-to-zero duobinary (RZ-DB), and return-to-zero alternate-mark-inversion (RZ-AMI). The CSRZ format shows an optical phase flip between adjacent pulses. In RZ-DB, a π-phase shift occurs whenever there are an odd number of 0-bits between two 1-bits; while for RZ-AMI the phase flips for each 1-bit, independent of the number of 0-bits in between. These four modulation formats show improved performances in high-speed optical systems relative to the conventional NRZ signal [22]–[26]. The RZ and CSRZ signals have been widely used in long-haul high-capacity wavelength division multiplexed (WDM) networks. RZ-AMI enables reduced nonlinear impairments through transmission, while RZ-DB shows narrow spectral width and thus enhanced tolerance to dispersion. In this paper, we test the four modulation formats through a silicon-microring resonator based delay line, and obtain error-free (BER $< 10^{-9}$) performances for the four modulation formats at 5-Gb/s signal rate. The maximal delay times at the error-free condition are 80, 95, 110, and 65 ps, for the RZ, CSRZ, RZ-DB, and RZ-AMI formats, respectively.

This paper is organized as follows. Section II presents the operating principle of a delay line based on ring resonator using

Manuscript received April 15, 2008; revised August 27, 2008. Current version published January 28, 2009. This work was supported in part by the National Science Foundation of China under Grant 60777040, the Shanghai Rising Star Program Phase II under Grant 07QH1400, and the Fok Ying Tung Fund under Grant 101067. The work of Z. Zhang and M. Qiu was supported by the Swedish Foundation for Strategic Research (SSF) through the Future Research Leader Program and by the Swedish Research Council (VR).

Q. Li, F. Liu, and Y. Su are with the State Key Laboratory of Advanced Optical Communication Systems and Networks, Department of Electronic Engineering, Shanghai Jiao Tong University, Shanghai 200240, China (e-mail: yikaisu@sjtu.edu.cn).

Z. Zhang and M. Qiu are with the Department of Microelectronics and Applied Physics, Royal Institute of Technology (KTH), 164 40 Kista, Sweden.

Color versions of one or more of the figures in this paper are available online at http://ieeexplore.ieee.org.

Digital Object Identifier 10.1109/JLT.2008.2005510

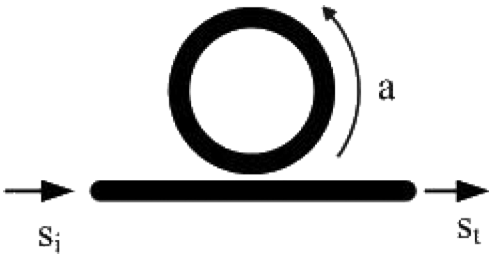

Fig. 1. Schematic of a ring resonator.

coupled mode theory. Section III describes the device characterization and experimental setup. Section IV demonstrates the system experimental results including the delayed eye diagrams, waveforms, and analysis of pattern dependency for the four modulation formats. Finally, conclusions are presented in Section V.

II. Operating Principle

The architecture of a ring resonator is shown in Fig. 1. It is a basic slow-light unit for any complicated CRS such as the APF and coupled-resonator optical waveguide (CROW) configurations [27]. While in most publications transfer matrix was employed to study the delay performances [28], here we use the coupled mode theory (CMT) to investigate the delay characteristics [29]. The analytic form of CMT can facilitate the analysis of cascaded slow-light CRS since a cascade of resonators coupled in series can be described by a set of coupled differential equations. Besides, the CMT can be used to model stopping light based on the bandwidth compression process in the CRS [30].

In the CMT, the ring is treated as an oscillator in time. Near the resonant frequency, the evolution of the electric field a inside a resonator which is coupled to a single-mode waveguide can be described by the CMT [29]

$$\frac{d}{dt}a = \left(j - \frac{1}{2Q_E} - \frac{1}{2Q_L}\right)\omega_0 a - j\sqrt{\frac{\omega_0}{Q_E}}s_i \qquad (1)$$

where ω_0 is the resonance frequency, Q_E and Q_L are the cavity quality factors related to external coupling and intrinsic cavity loss, respectively, and s_i is the incident waveguide field normalized such that its squared magnitude equals the incident power. The equation connecting the incident field s_i and transmitted field s_t can be expressed as follows:

$$s_t = s_i - j\sqrt{\frac{\omega_0}{Q_E}}a. \qquad (2)$$

After combining (1) and (2), the transmission function of the ring resonator can be expressed as

$$\frac{s_t}{s_i} = \frac{j\left(\frac{\omega-\omega_0}{\omega_0}\right) + \frac{1}{2Q_L} - \frac{1}{2Q_E}}{j\left(\frac{\omega-\omega_0}{\omega_0}\right) + \frac{1}{2Q_L} + \frac{1}{2Q_E}}. \qquad (3)$$

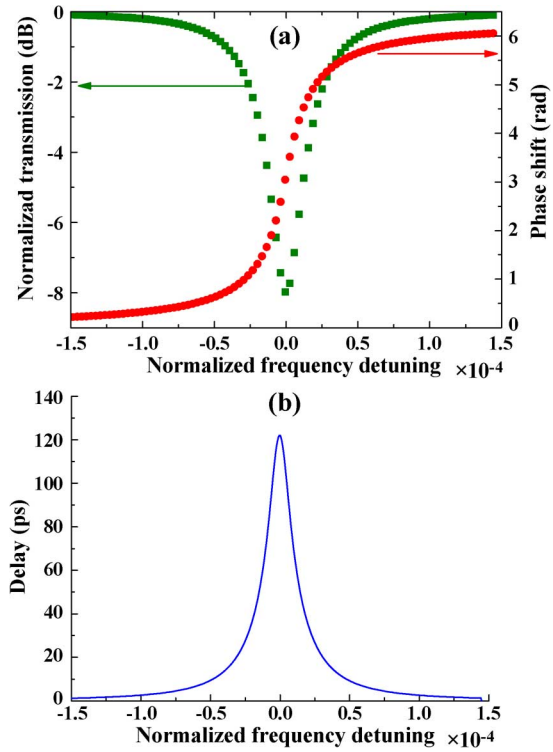

Fig. 2. Plot of (a) transmission and phase shift and (b) delay versus normalized frequency detuning for a ring resonator when Q_E and Q_L are 3.0×10^4 and 7.0×10^4, respectively, extracted from experimental measurements.

The transmission and phase shift characteristics for a ring resonator are related to the real part and imagery part of (3), respectively, and the group delay can be obtained by differentiating the phase shift with respect to the frequency. Fig. 2 shows the transmission, phase shift and delay versus the normalized frequency detuning for a ring resonator. The parameters used in simulations are the same as those in the experiment for the comparisons between the simulation and experimental results. The maximum group delay is ~120 ps on resonance. Since the group delay is wavelength dependent, optically tuneable delay lines can in practice be implemented by detuning resonators through thermal effect [31], electro-optical effect by carrier injection [32], electro-absorption effect [33], or other methods.

III. Device Characterisation and Experiment Setup

A. Silicon Microring Resonator

The microring resonator used in the experiments is fabricated on a commercial single-crystalline SOI wafer with a 250-nm-thick silicon slab on top of a 3-μm silica buffer layer to prevent the optical mode from leaking to the bottom handling wafer. The radius of the ring is 20 μm. The cross section of the silicon waveguide is 450 × 250 nm with an effective area of about 0.1 μm^2 for the transverse-electric (TE) mode. The microring is side coupled to the straight waveguide with an air gap of 120 nm. The waveguide and ring patterns are first defined in the electron beam lithography and then reactive ion plasma etching is performed to transfer the pattern to the silicon layer. The surface roughness is reduced by oxidizing 20 Å of silicon surfaces using wet chemistry. The waveguide is slowly tapered to a width of 10

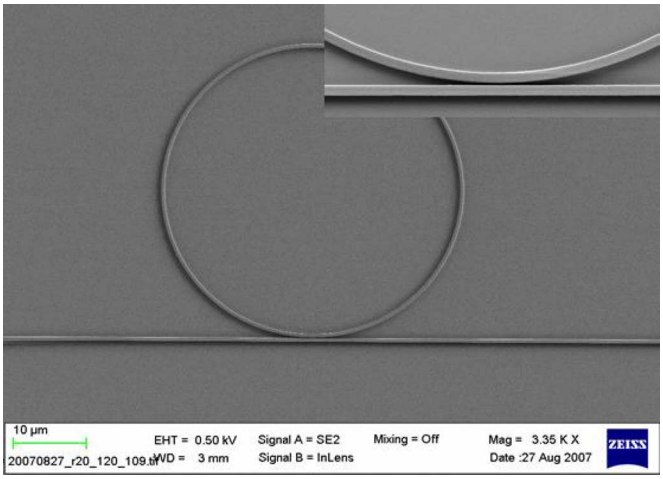

Fig. 3. SEM photographs of the silicon microring resonator with a radius of 20 μm. Inset is a zoom-in view of the coupling region.

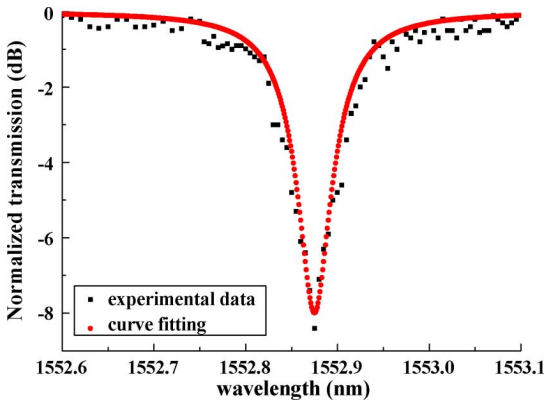

Fig. 4. Spectral response of the micro-ring resonator. The intrinsic Q_L is 7×10^4 and the coupling Q_E is 3×10^4.

μm at both ends, and then gold gratings are added to couple light near-vertically from single mode fibers [34]. This vertical coupling method possesses advantages in terms of easy alignment and simple fabrication of the mode converter compared to other coupling methods. With a period of 590 nm, a filling factor of 34% and a thickness of 25 nm, the grating couples only TE light with an minimal fiber-to-fiber loss below 20 dB. The scanning electron microscope (SEM) photos of the silicon microring resonator are provided in Fig. 3.

The spectral response of the microring resonator is shown in Fig. 4. The resonance at 1548.875 nm has a ~10-dB notch and the 3-dB bandwidth is ~0.1 nm. By fitting the measured spectral response with the transmission function given by (3), we obtain an intrinsic Q_L of 7.0×10^4 and a coupling Q_E of 3.0×10^4. Using the method presented in [35], we estimate that the coupling coefficient is ~0.27 and the loss is 10 dB/cm.

B. Experimental Setup

The experimental setup is depicted in Fig. 5. A single drive Mach–Zehnder modulator (MZM) is driven by a 5-Gb/s pseudorandom bit sequence (PRBS) signal with a length of $2^{15} - 1$ to generate NRZ format. A second MZM, which acts as a pulse

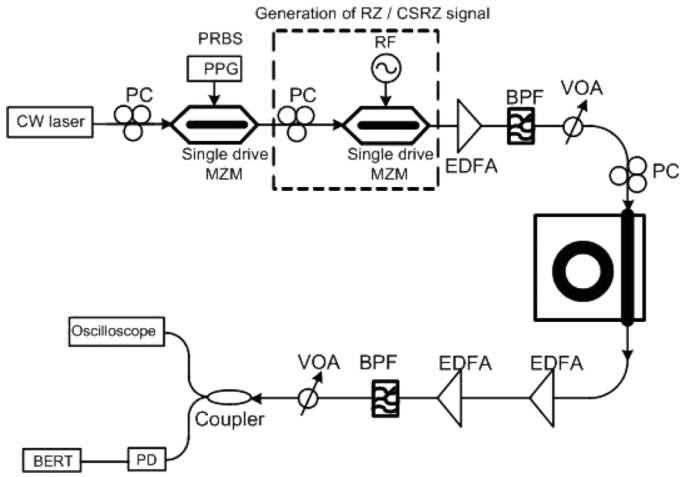

Fig. 5. Experimental setup. CW: continuous wave; PC: polarization controller; PPG: pulse pattern generator; MZM: Mach–Zehnder modulator; EDFA: erbium-doped fiber amplifier; BPF: bandpass filter; VOA: variable optical attenuator; PD: photodiode; BERT: BER tester.

carver, is sinusoidally driven by a synchronized radio-frequency (RF) signal to produce CSRZ or RZ signals, respectively. The first single dive MZM is replaced by a dual-drive MZM when generating RZ-DB and RZ-AMI signals [36]. The output signal is boosted by an erbium-doped fiber amplifier (EDFA) and then filtered by a tunable bandpass filter (BPF) with a bandwidth of 1.6 nm. The signal power injected into the fiber is controlled below 0 dBm to avoid nonlinear effect. As the gold grating is polarization-sensitive, a polarization controller is employed to make sure that the input light is in TE mode. The output signal of the microring resonator is amplified using two cascaded EDFAs and the noise is suppressed using a bandpass filter. Before the receiver, a variable optical attenuator (VOA) is used in order to tune the received optical power for the BER measurements. In the following measurements, all the results in eye diagram and power penalty have been defined at a BER of 10^{-9}.

IV. Experiment Results

In this section, we experimentally examine the delay characteristics of a ring resonator from the systematic point of view. Four typical modulation formats—RZ, CSRZ, RZ-DB and RZ-AMI signals are used and their delay performances and signal quality are characterized. In all the cases, the delay is defined by comparing the maximal eye-openings at different signal wavelengths.

A. RZ Data

First, we demonstrate error-free operation of the 5-Gb/s RZ signal. Fig. 6 shows the eye diagrams when off-resonance and on-resonance, respectively. The maximum delay is ~80 ps, corresponding to a fractional delay of ~0.4. The signal eye diagram is widely open, revealing good signal fidelity for the RZ signal. The power penalty increases with the delay. The BER of the RZ signal on-resonance shows only a sensitivity penalty of ~0.8 dB compared to the off-resonance case. Fig. 7 shows the dependence of the delay on the signal wavelength, demonstrating

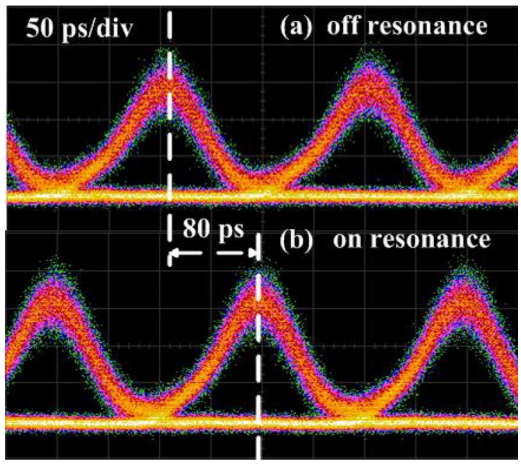

Fig. 6. Eye diagrams for the 5-Gb/s RZ signal when off resonance and on resonance, respectively.

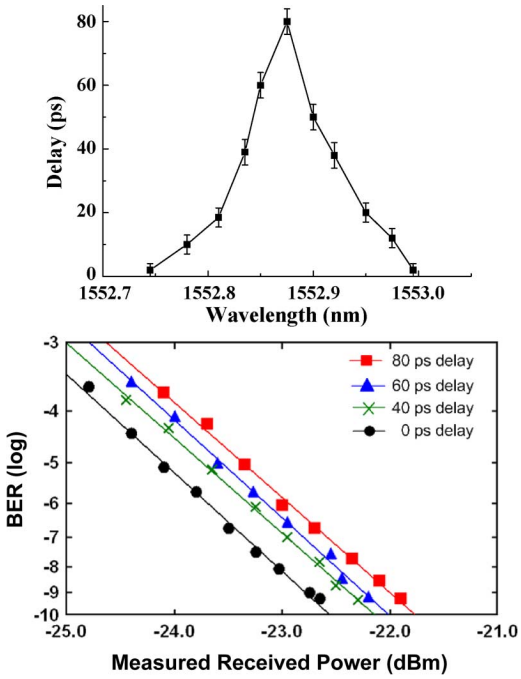

Fig. 7. Dependence of delay on signal wavelength and BER for the 5-Gb/s RZ signal.

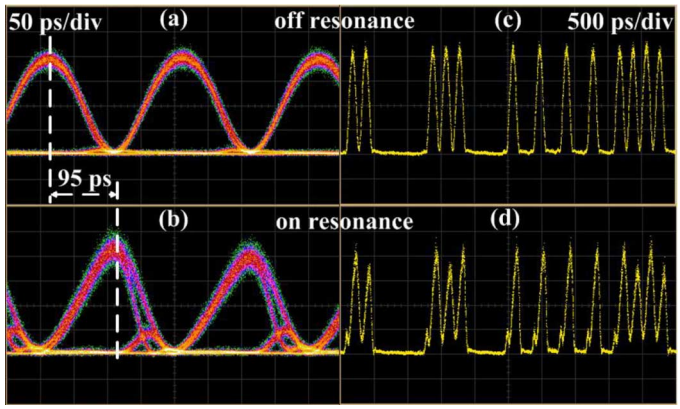

Fig. 8. Eye diagrams and waveforms for the 5-Gb/s CSRZ signal when off resonance and on resonance, respectively.

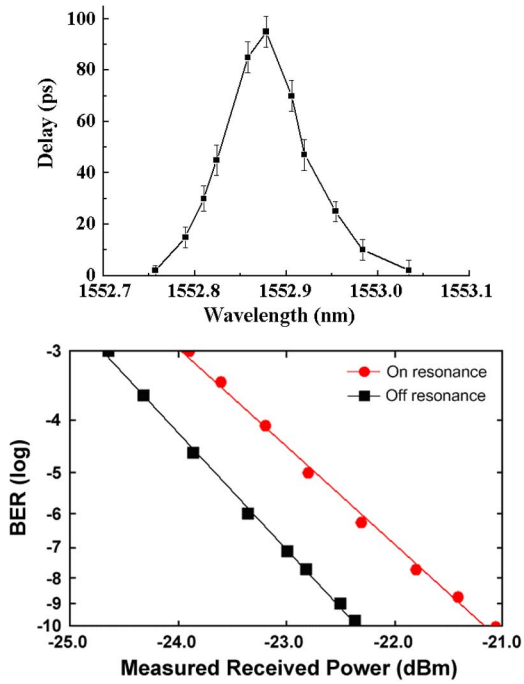

Fig. 9. Dependence of delay on signal wavelength and BER for the 5-Gb/s CSRZ signal when off resonance and on resonance, respectively.

that the delay is continuously tunable if the resonance of the microring can be tuned [31].

B. CSRZ Data

Fig. 8 provides the CSRZ eye diagrams and pulse pattern evolutions when off-resonance and on-resonance, respectively. The induced maximum delay on resonance is ∼95 ps and the corresponding fractional delay is ∼0.5. Due to the pattern dependence, the "1"-level fluctuations between two consecutive '1's with opposite phases appear in the eye diagram and the waveform, resulting in the signal degradation. The small ripples before each "1" bit are the consequence of the third order dispersion of the ring resonator when the signal is on resonance. Nevertheless, the eye diagram remains open. We measured the BER for the CSRZ signal when it is on resonance and off resonance, respectively, as illustrated in Fig. 9. The power penalty is ∼1.2 dB.

C. RZ-DB Data

Fig. 10 plots the eye diagrams and typical patterns for the 5-Gb/s RZ-DB signal when off-resonance and on-resonance, respectively. The obtained maximum delay is ∼110 ps, which is longer than half a bit. Also small ripples appear before each "1" bit due to the third order dispersion. In the RZ-DB, there is no pattern of adjacent 1's having opposite phases, while consecutive 1's can still cause "1"-level fluctuation, thus degrading the signal quality. From the BER curves shown in Fig. 11, a sensitivity penalty of ∼4.2 dB is observed for the RZ-DB signal on resonance.

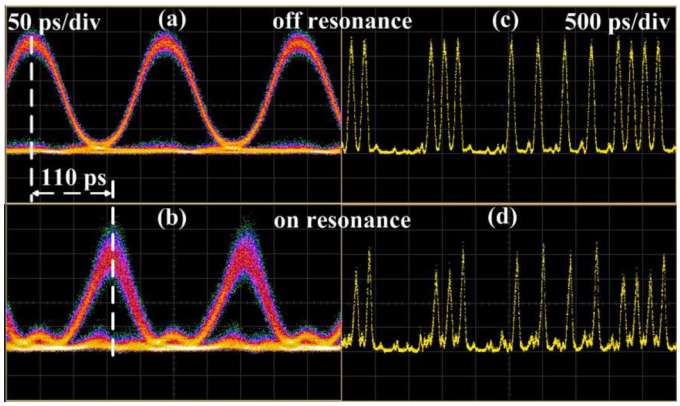

Fig. 10. Eye diagrams and waveforms for the 5-Gb/s RZ-DB signal when off resonance and on resonance, respectively.

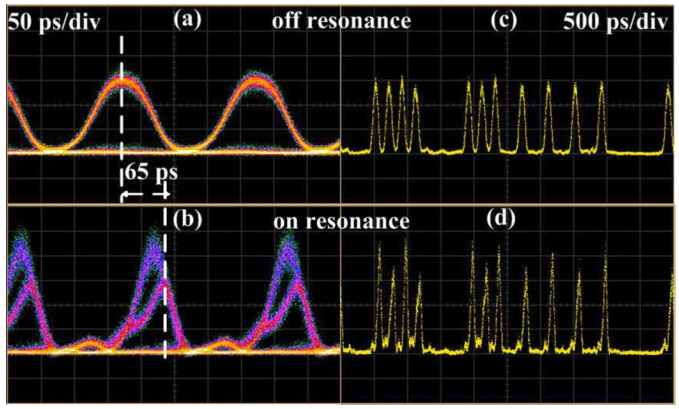

Fig. 12. Eye diagrams and waveforms for the 5-Gb/s RZ-AMI signal when off resonance and on resonance, respectively.

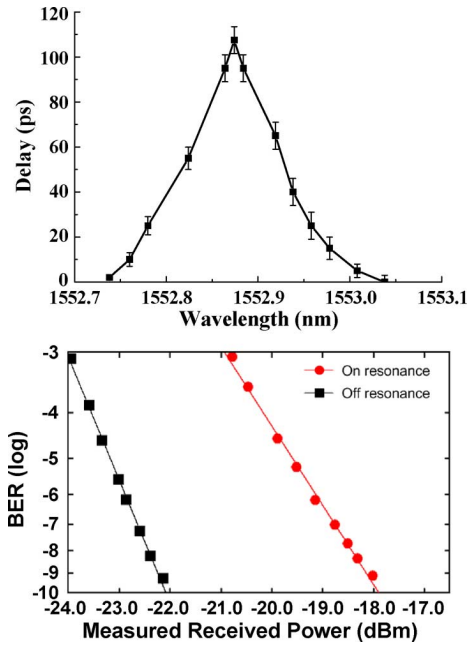

Fig. 11. Dependence of delay on signal wavelength and BER for the 5-Gb/s RZ-DB signal when off resonance and on resonance, respectively.

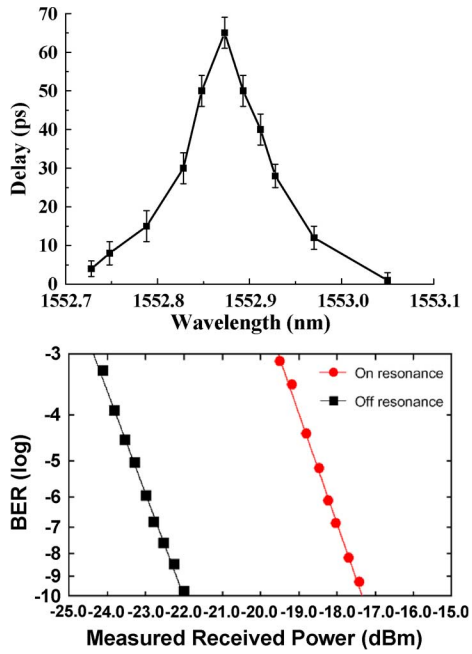

Fig. 13. Dependence of delay on signal wavelength and BER for the 5-Gb/s RZ-AMI signal when off resonance and on resonance, respectively.

D. RZ-AMI Data

For the 5-Gb/s RZ-AMI signal, the maximum delay is ∼65 ps, corresponding to a fractional delay of ∼0.35, as shown in Fig. 12. More severe eye closure is observed, and the BER measurements in Fig. 13 show a larger sensitivity penalty of ∼4.6 dB when the signal is on resonance.

E. Discussion

1) Delay Analysis: From the above measurements, the maximum group delays for the 5-Gb/s RZ, CSRZ, RZ-DB and RZ-AMI signals are 80 ps, 95 ps, 110 ps and 65 ps, respectively. The 110-ps group delay obtained for the RZ-DB signal is very close to the predicted maximum value (∼120 ps) according to the CMT analysis provided in Section II. Following the RZ-DB are the CSRZ, RZ, and RZ-AMI in maximum delay values. This can be explained by their optical spectral features, as plotted in Fig. 14. For the RZ-DB signal, it exhibits a much narrower bandwidth compared with the other three modulation formats. The spectral compactness of RZ-DB signal enables that most of its components match the resonance and thus experience the maximum group delay. For the RZ-AMI signal, the carrier on the resonance frequency is completely suppressed while two sidebands carrying the signal experience less delay, thus leading to a decreased group delay. For the RZ and CSRZ signals, their spectral widths are between the RZ-DB and RZ-AMI formats, thus showing moderate group delays.

2) Distortion Analysis: On the signal quality, the ring-resonator bandwidth is not a major limiting factor since it is larger than the signal bandwidth. The signal degradations mainly result from two factors: 1) dispersion and 2) data pattern dependence. While the waveguide itself is assumed to be dispersion-free, strong dispersive effects are induced by the resonant process. Fig. 15 depicts the group velocity (GVD) and third order dispersion (TOD) curves for the ring resonator. While the GVD is zero on resonance, strong normal or anomalous dispersion can

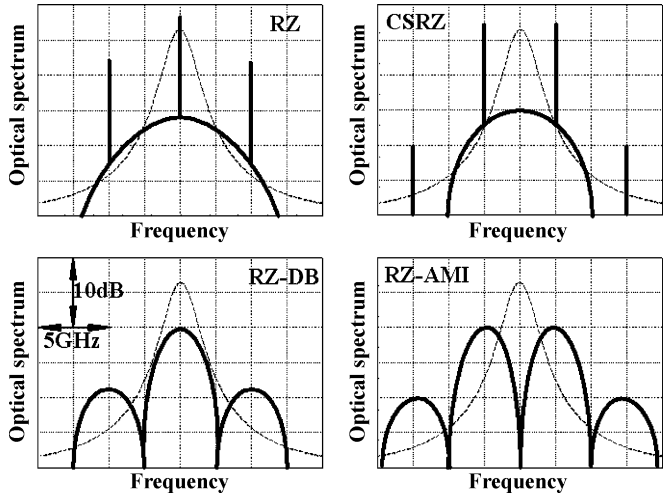

Fig. 14. Optical spectra for the four modulation formats. The dashed curves representing the relative group delays are from Fig. 2(b).

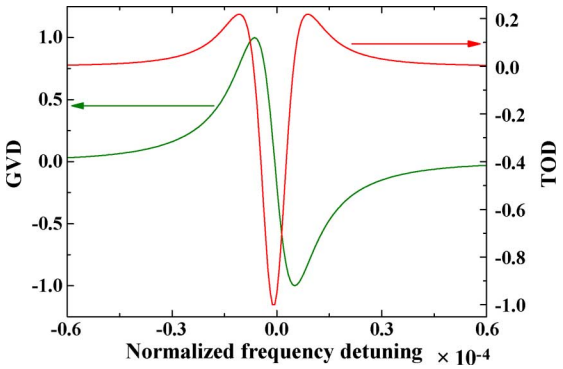

Fig. 15. Functional dependence of the GVD and TOD on the normalized frequency detuning for a ring resonator when Q_E and Q_L are 3.0×10^4 and 7.0×10^4, respectively. The GVD and TOD are normalized to the maxima.

be obtained on the red or blue side of the resonance, respectively. The TOD achieves the maxima on resonance and is the main dispersion contribution to the signal distortion [27]. The ripples appear before each "1" bit, which were observed in the delayed CSRZ, RZ-DB and RZ-AMI signals, are related with the negative third-order dispersion on resonance [9], [37].

We simulated the delayed signal waveforms on resonance at data rates of 2.5, 5.0, 7.5, and 10 Gb/s, respectively, shown in Fig. 16. For a given resonance width, as the bit rate increases, the oscillations appearing near the trailing edge of the pulse become obvious. When the data rate is pushed to the limitation of the resonance bandwidth (~7.5 GHz), the oscillations induced by the TOD severely degrade the delayed-signal quality. Therefore, the TOD is a major factor limiting the available bandwidth of the ring-resonator based delay line.

The phase-modulation scheme associated with certain data patterns plays a key role in signal quality. Two major degrading factors are: 1) interaction between two consecutive 1's with opposite phase, namely the "1 −1" pattern and 2) level fluctuation for consecutive 1's with the same phase, i.e., the "1 1" pattern [17]. For the CSRZ and RZ-AMI signals, the 1 −1 is a typical pattern and there is no 1 1 pattern, two consecutive 1's with opposite phases destructively interact with each other and thus lead to the 1-level fluctuation and degrade the signal quality. For the

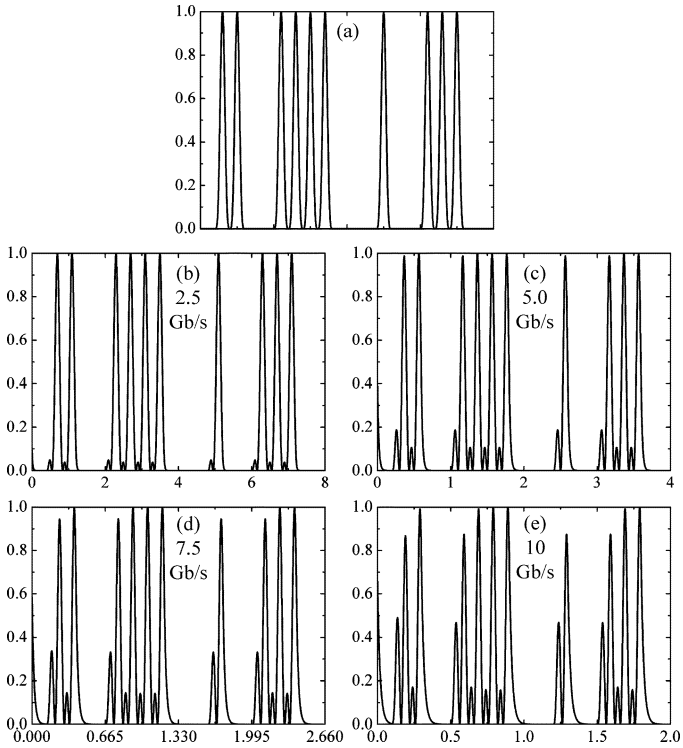

Fig. 16. Simulation results of delayed signal waveforms when signal on resonance at 2.5, 5.0, 7.5, and 10 Gb/s, respectively. The parameters of the ring resonator are identical to those of the fitted spectrum in Fig. 4. Horizontal axis: time (unit: ns); vertical axis: normalized intensity.

RZ-DB signal where no 1 −1 pattern exists, the 1 1 is a typical pattern that contributes to the 1-level fluctuation.

The power penalties on resonance for RZ, CSRZ, RZ-DB and RZ-AMI are ~0.8, ~1.2, ~4.2, and ~4.6 dB, respectively. The power penalties come from the signal degradations owing to the TOD and pattern-dependent phase modulations. The RZ-DB and RZ-AMI have large power penalties due to their relatively large fluctuations in the "1" level caused by pattern-dependent phase modulations, as shown in their delayed eye diagrams.

3) Delay-Bandwidth Product Analysis: For a signal ring resonator, the maximum delay on resonance is given by [27]

$$T_D = \frac{(1-r^2)a}{(a-r)(1-ra)}\tau_d \tag{4}$$

where a represents the single-pass amplitude transmission related to Q_L, r is the reflective coefficient related to Q_E, and τ_d is the single-pass delay.

We use the 3-dB spectral width to characterize the bandwidth of this delay line. It requires that the main lobe of the power spectrum of the modulated signal should be smaller than the 3-dB spectral width Δf_{FWHM}, which is given by [27]

$$\Delta f_{\mathrm{FWHM}} = \frac{(1-ar)}{\pi\sqrt{ar}}\frac{1}{\tau_d}. \tag{5}$$

Thus, the delay bandwidth product can be denoted as

$$\Delta f_{\mathrm{FWHM}} T_D = \sqrt{\frac{a}{r}}\frac{(1-r^2)}{\pi(a-r)} \xrightarrow{a=1} \frac{(1+r)}{\pi\sqrt{r}} \simeq \frac{2}{\pi}. \tag{6}$$

In our case, the resonance of the microring has a 3-dB bandwidth of ∼0.06 nm (∼7.5 GHz). The RZ-DB signal achieves the maximum delay-bandwidth product (∼0.55).

V. Conclusion

We have theoretically studied the delay characteristics of a silicon ring resonator based on CMT. We then experimentally demonstrated error-free operations of an SOI ring-resonator delay line for 5-Gb/s signals with different modulation formats, including RZ, CSRZ, RZ-DB, and RZ-AMI signals. The maximal delay times with error-free operations are 80 ps, 95 ps, 110 ps and 65 ps, respectively, corresponding to a fractional group delay of ∼0.4, ∼0.5, ∼0.55, and ∼0.35. The differences in group delay mainly result from spectral features of the different formats, while the pulse distortions are related with the pattern dependences. The third-order dispersion of the resonator is a main contributing factor to the signal degradation when on resonance. Since a single microring resonator is the building block for more complicated slow-light CRS such as the APF and CROW configurations, we believe that our analysis and demonstrations can be extended to these slow-light CRS.

References

[1] C. J. Chang-Hasnain, P. C. Ku, J. Kim, and S. L. Chuang, "Variable optical buffer using slow light in semiconductor nanostructures," *Proc. IEEE*, vol. 91, no. 11, pp. 1884–1897, Nov. 2003.

[2] W. Zhong and R. S. Tucker, "Wavelength routing-based photonic packet buffers and their applications in photonic packet switching systems," *J. Lightw. Technol.*, vol. 16, no. 10, pp. 1737–1745, Oct. 1998.

[3] R. Boyd, D. Gauthier, and A. Gaeta, "Applications of slow-light in telecommunications," *Opt. Photon. News*, vol. 17, no. 4, pp. 19–23, Apr. 2006.

[4] B. Zhang, L. Zhang, L. S. Yan, I. Fazal, J. Y. Yang, and A. E. Willner, "Continuously-tunable, bit-rate variable OTDM using broadband SBS slow-light delay line," *Opt. Exp.*, vol. 15, no. 13, pp. 8317–8322, Jun. 2007.

[5] B. Zhang, L. S. Yan, J. Y. Yang, I. Fazal, and A. E. Willner, "A single slow-light element for independent delay control and synchronization on multiple Gb/s data channels," *IEEE Photon. Technol. Lett.*, vol. 19, no. 14, pp. 1081–1083, Jul. 2007.

[6] J. Scheuer, G. T. Paloczi, J. Poon, and A. Yariv, "Coupled resonator optical waveguides: Toward the slowing and storage of light," *Opt. Photon. News*, vol. 16, no. 2, pp. 36–40, Feb. 2005.

[7] Y. Tanaka, J. Upham, T. Nagashima, T. Sugiya, T. Asano, and S. Noda, "Dynamic control of the Q factor in a photonic crystal nanocavity," *Nature Mater.*, vol. 6, no. 11, pp. 862–865, Nov. 2007.

[8] J. K. S. Poon, L. Zhu, G. A. D. Rose, and A. Yariv, "Transmission and group delay of microring coupled-resonator optical waveguides," *Opt. Lett.*, vol. 31, no. 4, pp. 456–458, Feb. 2006.

[9] F. Morichetti, A. Melloni, A. Breda, A. Canciamilla, C. Ferrari, and M. Martinelli, "A reconfigurable architecture for continuously variable optical slow-wave delay lines," *Opt. Exp.*, vol. 15, no. 25, pp. 17273–17282, Dec. 2007.

[10] J. Yang, A. O. Karalar, S. S. Djordjevic, N. K. Fontaine1, C. Yang, W. Chen, S. Chu, B. E. Little, and S. J. B. Yool, "Variable slowlight buffers in all-optical packet switching routers," presented at the Proc. OFC, Anaheim, CA, 2008, Paper OTuF2E, unpublished.

[11] B. Jalali and S. Fathpour, "Silicon photonics," *J. Lightw. Technol.*, vol. 24, no. 12, pp. 4600–4615, Dec. 2006.

[12] G. T. Reed, "The optical age of silicon," *Nature*, vol. 427, no. 6975, pp. 595–596, Feb. 2004.

[13] M. Lipson, "Guiding, modulating, and emitting light on silicon—Challenges and opportunities," *J. Lightw. Technol.*, vol. 23, no. 12, pp. 4222–4238, Dec. 2005.

[14] B. Jalali, "Teaching silicon new tricks," *Nature Photon.*, vol. 1, no. 4, pp. 193–195, Apr. 2007.

[15] R. Soref, "The past, present and future of silicon photonics," *IEEE J. Sel. Topics Quantum Electron.*, vol. 12, no. 6, pp. 1678–1687, Nov./Dec. 2006.

[16] F. Xia, L. Sekaric, and Y. Vlasov, "Ultracompact optical buffers on a silicon chip," *Nature Photon.*, vol. 1, no. 1, pp. 65–71, Jan. 2007.

[17] F. Liu, Y. Su, and P. L. Voss, "Optimal operating conditions and modulation format for 160 Gb/s signals in a fiber parametric amplifier used as a slow-light delay line element," presented at the Proc. OFC, Anaheim, CA, 2007, paper OWB5, unpublished.

[18] P. J. Winzer and R. J. Essiambre, "Advanced optical modulation formats," *Proc. IEEE*, vol. 94, no. 5, pp. 952–985, May 2006.

[19] B. Zhang, L. Yan, I. Fazal, L. Zhang, A. E. Willner, Z. Zhu, and D. J. Gauthier, "Slow light on Gbit/s differential-phase-shift-keying signals," *Opt. Exp.*, vol. 15, no. 4, pp. 1878–1883, Feb. 2007.

[20] B. Zhang, L. Yan, L. Zhang, S. Nuccio, L. Christen, T. Wu, and A. E. Willner, "Spectrally efficient slow light using multilevel phase-modulated formats," *Opt. Lett.*, vol. 33, no. 1, pp. 55–57, Jan. 2008.

[21] L. Zhang, T. Luo, C. Yu, W. Zhang, and A. E. Willner, "Pattern dependence of data distortion in slow-light elements," *J. Lightw. Technol.*, vol. 25, no. 7, pp. 1754–1760, Jul. 2007.

[22] K. S. Cheng and J. Conradi, "Reduction of pulse-to-pulse interaction. using alternative RZ formats in 40-Gb/s systems," *IEEE Photon. Technol. Lett.*, vol. 14, no. 1, pp. 98–100, Jan. 2002.

[23] A. H. Gnauck, X. Liu, X. Wei, D. M. Gill, and E. C. Burrows, "Comparison of modulation formats for 42.7-Gb/s single-channel transmission through 1980 km of SSMF," *IEEE Photon. Technol. Lett.*, vol. 16, no. 3, pp. 909–911, Mar. 2004.

[24] A. Agarwal, S. Banerjee, D. F. Grosz, A. P. Küng, D. N. Maywar, A. Gurevich, and T. H. Wood, "Ultra-high-capacity long-haul 40-Gb/s WDM transmission with 0.8-b/s/Hz spectral efficiency by means of strong optical filtering," *IEEE Photon. Technol. Lett.*, vol. 15, no. 3, pp. 470–472, Mar. 2003.

[25] C. Xie, L. Möller, and R. Ryf, "Improvement of optical NRZ- and RZ-duobinary transmission systems with narrow bandwidth optical filters," *IEEE Photon. Technol. Lett.*, vol. 16, no. 9, pp. 2162–2164, Sep. 2004.

[26] Y. Lu and Y. Su, "Conversions among binary optical modulation formats," *Opt. Exp.*, vol. 16, no. 6, pp. 3853–3858, Mar. 2008.

[27] J. E. Heebner, "Nonlinear optical whispering gallery microresonators for photonics" Ph.D. dissertation, Inst. of Optics, Univ. of Rochester, Rochester, NY [Online]. Available: http://www.optics.rochester.edu/workgroups/boyd/nonlinear.html

[28] J. E. Heebner and R. W. Boyd, "'Slow' and 'fast' light in resonator coupled waveguides," *J. Mod. Opt.*, vol. 49, no. 14/15, pp. 2629–2636, Nov. 2002.

[29] B. E. Little, S. T. Chu, H. A. Haus, J. S. Foresi, and J. P. Laine, "Microring resonator channel dropping filters," *J. Lightw. Technol.*, vol. 15, no. 6, pp. 99–1005, Jun. 1997.

[30] M. F. Yanik and S. Fan, "Stopping light all optically," *Phys. Rev. Lett.*, vol. 92, no. 8, p. 083901, Feb. 2004.

[31] F. Liu, Q. Li, Z. Zhang, M. Qiu, and Y. Su, "Optically tunable delay line in silicon microring resonator based on thermal nonlinear effect," *IEEE J. Sel. Topics Quantum Electron.*, vol. 14, no. 3, pp. 706–712, May/Jun. 2008.

[32] Q. Xu, B. Schmidt, S. Pradhan, and M. Lipson, "Micrometre-scale silicon electro-optic modulator," *Nature*, vol. 435, no. 7040, pp. 325–327, May 2005.

[33] T. Liang, L. Nunes, T. Sakamoto, K. Sasagawa, T. Kawanishi, M. Tsuchiya, G. Priem, D. Van Thourhout, P. Dumon, R. Baets, and H. Tsang, "Ultrafast all-optical switching by cross-absorption modulation in silicon wire waveguides," *Opt. Exp.*, vol. 13, no. 19, pp. 7298–7303, Sep. 2005.

[34] S. Scheerlinck, J. Schrauwen, F. Van Laere, D. Taillaert, D. Van Thourhout, and R. Baets, "Efficient, broadband and compact metal grating couplers for silicon-on-insulator waveguides," *Opt. Exp.*, vol. 15, no. 15, pp. 9639–9644, Jul. 2007.

[35] C. Manolatou and M. Lipson, "All-optical silicon modulators based on carrier injection by two-photon absorption," *J. Lightw. Technol.*, vol. 24, no. 3, pp. 1433–1439, Mar. 2006.

[36] F. T. Hansen, P. B. Nielsen, and T. N. Eskildsen, "Duobinary transmitter with low intersymbol interference," *IEEE Photon. Technol. Lett.*, vol. 10, no. 4, pp. 597–599, Apr. 1998.

[37] G. P. Agrawal, *Nonlinear Fiber Optics*, 3rd ed. San Diego, CA: Academic, 2001.

Qiang Li (S'07) received the B.S. and M.S. degrees from Harbin Institute of Technology, Harbin, China, in 2005 and 2007, respectively. He is currently working toward the Ph.D. degree at Shanghai Jiao Tong University, Shanghai, China.

His research interests include slow-light delay line and storage and optical information processing in silicon waveguides.

Fangfei Liu (S'07) received the B.S. degree in electronic engineering from Shanghai Jiao Tong University, Shanghai, China, in 2007, where she is currently working toward the M.S. degree in electronic engineering.

Her research interests include advanced modulation formats for high-speed optical communication systems, nonlinear optics in waveguides and fibers, and optical signal processing.

Ms. Liu was the recipient of the National Mathematical Modeling Contest in China in 2005.

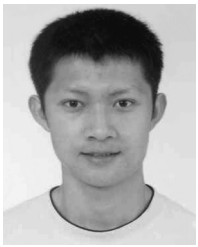

Ziyang Zhang received the B.S. degree in optical engineering from Zhejiang University, Hangzhou, China, in 2003 and the M.S. degree in photonics and the Ph.D. degree from the Royal Institute of Technology (KTH), Kista, Sweden, in 2004 and 2008, respectively.

He is currently a Post-doctoral Researcher with the Heinrich-Hertz Institute, Berlin, Germany. His research area extends from silicon photonics to polymer-based photonic integrated circuits.

Min Qiu (M'99) received the B.Sc. degree and Ph.D. degree in condense matter physics from Zhejiang University, Hangzhou, China, in 1995 and 1999, respectively, and the Ph.D. degree in electromagnetic theory from the Royal Institute of Technology (KTH), Stockholm, Sweden, in 2001.

In 2001, he joined the Department of Microelectronics and Applied Physics, Royal Institute of Technology (KTH), Kista, Sweden, where he is currently an Associate Professor. He is the author or coauthor of more than 80 international refereed journal papers and more than 60 conference contributions. His research interests include optical metamaterials, photonic crystals, plasmonic optics, and integrated optical circuits.

Dr. Qiu is a member of the Optical Society of America and the European Optical Society. He was the recipient of the Individual Grant of "Future Research Leader" (INGVAR) from the Swedish Foundation for Strategic Research (SSF) in 2004. He is also currently holding a Senior Researcher Fellowship from Swedish Research Council.

Yikai Su (M'01–SM'07) received the B.S. degree from the Hefei University of Technology, Hefei, China, in 1991, the M.S. degree from the Beijing University of Aeronautics and Astronautics, Beijing, China, in 1994, and the Ph.D. degree in electrical engineering from Northwestern University, Evanston, IL, in 2001.

He was with Crawford Hill Laboratory, Bell Laboratories, for three years before joining Shanghai Jiao Tong University, Shanghai, China, as a Full Professor in 2004. He became the Associate Department Chair of Electronic Engineering in 2006. His research areas cover modulation formats, optical signal processing, and silicon nanophotonic devices. He has authored or coauthored approximately 150 publications in prestigious international journals and conferences, including approximately 40 IEEE PHOTONICS TECHNOLOGY LETTERS papers, more than 20 invited conference presentations, and eight postdeadline papers. He holds four U.S. patents with over 10 U.S. or Chinese patents pending.

Prof. Su is a member of the Optical Society of America. He also serves as the Chair of IEEE ComSoc Shanghai Chapter, and a faculty advisor of OSA student chapter in Shanghai Jiao Tong University. He serves as a Topical Editor of *Optics Letters,* was a Guest Editor of the IEEE JOURNAL ON SELECTED TOPICS IN QUANTUM ELECTRONICS on "Nonlinear Optical Signal Processing," a Co-Chair of Workshop on Optical Transmission and Equalization (WOTE) 2005, ChinaCom2007 Symposium, IEEE/OSA AOE 2007 Slow Light Workshop, Asia Pacific Optical Communications (APOC) 2008 SC3, and a Technical Committee Member of Opto-Electronics and Communications Conference (OECC) 2008, the Conference on Laser and Electro-Optics (CLEO) Pacific Rim (PR) 2007, IEEE Lasers and Electro-Optics Society (LEOS) Summer Topical Meeting 2007 on Ultra-High-Speed Transmission, IEEE Lasers and Electro-Optics Society (LEOS) 2005–2007, BroadNets2006, the Asia-Pacific Optical Communications (APOC) Conference 2005, and the International Conference on Optical Communications and Networks (ICOCN) 2004.